

# Green Light-Excitable Ce-Doped Nitridomagnesoaluminate Sr[Mg<sub>2</sub>Al<sub>2</sub>N<sub>4</sub>] Phosphor for White Light-Emitting Diodes

Julius L. Leaño, Jr.,<sup>†,‡,§,||</sup> Shin-Ying Lin,<sup>†,‡</sup> Agata Lazarowska,<sup>⊥</sup> Sebastian Mahlik,<sup>⊥</sup> Marek Grinberg,<sup>⊥</sup> Chaolun Liang,<sup>#,∇</sup> Wuzong Zhou,<sup>#</sup> Maxim S. Molokeyev,<sup>○,⊗</sup> Victor V. Atuchin,<sup>¶,Ⓛ,Ⓟ,★,◆</sup> Yi-Ting Tsai,<sup>‡</sup> Chun Che Lin,<sup>‡</sup> Hwo-Shuenn Sheu,<sup>♠</sup> and Ru-Shi Liu<sup>\*,‡,‡,◆</sup>

<sup>‡</sup>Department of Chemistry, National Taiwan University, Taipei 106, Taiwan

<sup>§</sup>Nanoscience and Technology Program, Taiwan International Graduate Program, Academia Sinica and National Taiwan University, Taipei 115, Taiwan

<sup>||</sup>Department of Science and Technology, Philippine Textile Research Institute, Taguig City 1631, Philippines

<sup>⊥</sup>Institute of Experimental Physics, University of Gdansk, Wita Stwosza 57, 80-952 Gdansk, Poland

<sup>#</sup>EaStCHEM, School of Chemistry, University of St Andrews, St Andrews, Fife KY16 9ST, United Kingdom

<sup>∇</sup>Instrumental Analysis & Research Center, Sun Yat-sen University, Guangzhou 510275, China

<sup>○</sup>Laboratory of Crystal Physics, Kirensky Institute of Physics, SB RAS, Krasnoyarsk 660036, Russia

<sup>⊗</sup>Department of Physics, Far Eastern State Transport University, Khabarovsk 680021, Russia

<sup>¶</sup>Laboratory of Optical Materials & Structures, Institute of Semiconductor Physics, SB RAS, Novosibirsk 630090, Russia

<sup>Ⓛ</sup>Functional Electronics Laboratory, Tomsk State University, Tomsk 634050, Russia

<sup>★</sup>Laboratory of Semiconductor and Dielectric Materials, Novosibirsk State University, Novosibirsk 630090, Russia

<sup>◆</sup>Institute of Chemistry, Tyumen State University, Tyumen 525003, Russia

<sup>♠</sup>National Synchrotron Radiation Research Center, Hsinchu 300, Taiwan

<sup>Ⓛ</sup>Department of Mechanical Engineering and Graduate Institute of Manufacturing Technology, National Taipei University of Technology, Taipei 106, Taiwan

## Supporting Information

Efficiency in the conversion of electrical energy to light has been a paramount consideration in the search and development of energy-saving alternatives to conventional incandescent bulbs.<sup>1</sup> Phosphor-converted white light-emitting diodes (pc-WLEDs) have emerged as a promising technology to revolutionize modern day lighting. This technology ensures energy-efficiency and improves color rendition and luminous efficacies.<sup>1</sup>

A novel class of nitride of groups III and IV has been reported to have remarkable luminescence properties with Eu<sup>2+</sup> as activator. These remarkable intense emissions ascribed to the 4f<sup>6</sup>(<sup>7</sup>F)5d<sup>1</sup> to 4f<sup>7</sup>(<sup>8</sup>S<sub>7/2</sub>) transitions are manifested in the entire range of the visible spectrum.<sup>2</sup> These new and structurally related phosphor materials offer a robust platform toward red-emitting phosphors and thus provide an opportunity to improve color rendition of pc-LEDs. These newly reported narrow-band red phosphors result in high color rendition and significantly increased luminous efficacies for as-fabricated white LED devices. Moreover, these UC<sub>4</sub>C<sub>4</sub>-type compounds can also accommodate Ce<sup>3+</sup> into the host lattice, which produces the characteristic emission.<sup>3</sup> Recently, novel isotypic nitridomagnesoaluminates M[Mg<sub>2</sub>Al<sub>2</sub>N<sub>4</sub>] (M = Ca, Sr, Ba, Eu) have been prepared in a radiofrequency furnace using fluoride starting materials. The anionic networks of (Al/Mg)N<sub>4</sub> are connected together by common edges and corners, thereby generating a highly condensed disordered framework, where the cation site is in the middle of *vierer*<sup>2</sup> ring channels along

[001] and forms a cuboid coordination environment.<sup>4</sup> The cuboid site in this class of nitride phosphors offers an opportunity for narrow-band emission that has huge advantages for practical applications. New phosphors are developed through several strategies, including chemical unit cosubstitution which has been successfully employed in finding new solid-state materials.<sup>5,6</sup> Herein, we report a yellow-emitting Ce-doped Sr[Mg<sub>2</sub>Al<sub>2</sub>N<sub>4</sub>] phosphor synthesized using all-nitride starting materials via gas pressure sintering (GPS). Its application as a component of a pc-LED package fabricated through a unique configuration is a promising approach to generate white light.

GPS is a simple approach toward the development and up-scale phosphor synthesis. The Sr<sub>1-x</sub>[Mg<sub>2</sub>Al<sub>2</sub>N<sub>4</sub>]:Ce<sub>x</sub><sup>3+</sup> series was prepared from all-nitride (Sr<sub>3</sub>N<sub>2</sub>, Mg<sub>3</sub>N<sub>3</sub>, AlN, and CeN) precursors were loaded in Mo crucibles prior to sintering at 1450 °C for 4 h under 0.9 MPa N<sub>2</sub> atmosphere. Varying the amount of Ce<sup>3+</sup> from *x* = 0.005–0.08 yielded a light pink colored product that emitted yellow light under UV (Figure S1). The synthesized phosphor correlated very well with CSD-425321 (Figure S2). Rietveld refinement revealed that almost all the peaks except for those of AlN (wt. ~12.2(3)%) were in a tetragonal crystal system with *I4/m* (No. 87) space group (Figure 1a). The crystallographic data of

Received: August 17, 2016

Revised: September 21, 2016

Published: September 25, 2016

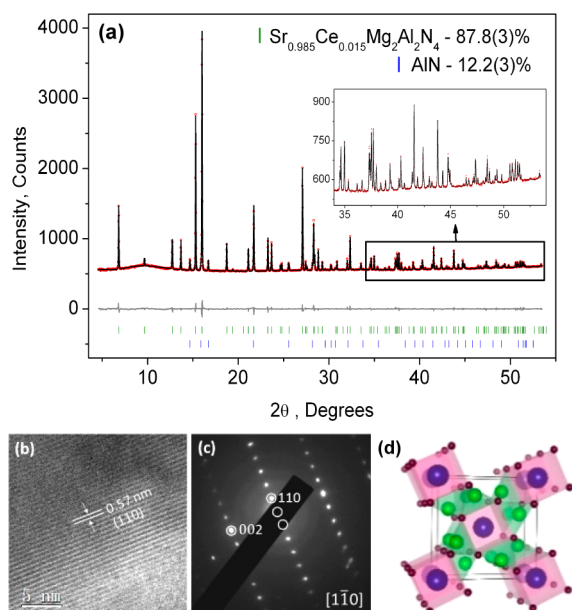


**Figure 1.** GPS-synthesized  $\text{Sr}[\text{Mg}_2\text{Al}_2\text{N}_4]:\text{Ce}^{3+}$  (a) Rietveld refinement of the XRD patterns of  $\text{Sr}_{0.985}(\text{Mg}_2\text{Al}_2\text{N}_4):\text{Ce}_{0.015}$ , observed (black line), calculated (red circles), difference (gray)  $\text{Sr}_{0.985}[\text{Mg}_2\text{Al}_2\text{N}_4]:\text{Ce}_{0.015}$  (green) and AlN (blue). (b) HRTEM image; (c) SAED pattern indexed to the tetragonal unit cell. (d) Crystal structure of  $\text{Sr}[\text{Mg}_2\text{Al}_2\text{N}_4]:\text{Ce}^{3+}$  viewed along the  $b$ -direction (blue spheres,  $\text{Sr}^{2+}$ ; green spheres,  $\text{Al}^{3+}$  or  $\text{Mg}^{2+}$ ; red spheres,  $\text{N}^{3-}$ ; green tetrahedra, four N-coordinated Al/Mg sites; blue cuboid, eight N-coordinated  $\text{Sr}^{2+}/\text{Ce}^{3+}$  site).

$\text{Sr}_{0.985}\text{Mg}_2\text{Al}_2\text{N}_4:\text{Ce}_{0.015}^{3+}$  reveal  $a = 8.17648(8)$  and  $c = 3.35754(4)$  Å parameters (Table S1), which are comparable to the  $\text{SrMg}_2\text{Al}_2\text{N}_4$  prepared using a radiofrequency synthetic approach (Table S2).<sup>5</sup>

Occupancies of  $\text{Mg}^{2+}$  and  $\text{Al}^{3+}$  ions were refined with the assumption that the sum of their occupancies is equal to 1. The concentration of  $\text{Ce}^{3+}$  in the  $\text{Sr}^{2+}$  site was not refined but was fixed according to the chemical formula due to its relatively small value. Refinement gave low  $R$ -factors (Table S1), and the coordinates of atoms and main bond lengths are shown in Tables S3 and S4. The elemental ratio of the elements from the EDS data (Figure S3) is in good agreement with the sum formula. In the crystal structure (Figure 1d), disordered (Mg/Al) $\text{N}_4$  forms strands of edge-sharing tetrahedral that creates *vierer* rings along [001], which are also seen in the crystal structure of  $M[\text{Mg}_2\text{Al}_2\text{N}_4]$  ( $M = \text{Ca}, \text{Sr}, \text{Ba}, \text{Eu}$ ).<sup>5</sup> The  $\text{Sr}^{2+}$  ions are found in every second *vierer* ring channel that forms an 8-nitrogen coordinated cuboid site.<sup>2</sup> This cuboid coordination site is a feature of  $\text{UCr}_4\text{C}_4$ -structures<sup>6</sup> that distinctly give rise to a 3D-network of (Mg/Al) $\text{N}_4$  tetrahedra, and  $\text{Sr}[\text{Mg}_2\text{Al}_2\text{N}_4]:\text{Ce}^{3+}$  shares this structural similarity with other nitridolithoaluminates.<sup>2</sup> Figure 1b and 1c show the high-resolution transmission electron microscopy (HRTEM) image and corresponding select area electron diffraction (SAED) pattern of  $\text{Sr}_{0.985}\text{Mg}_2\text{Al}_2\text{N}_4:\text{Ce}_{0.015}^{3+}$ , respectively. However, careful control of TEM conditions allows the structure to remain intact under the electron beam for up to 10 min.<sup>7</sup> The distinct lattice fringes of 0.57 nm in Figure 1b corresponds to the (110) planes of the tetragonal structure. The AlN minor phase was also detected, but its structure is different (Figure S3).

The photoluminescence excitation (PLE) and photoluminescence (PL) measured at room temperature are shown in Figure 2a,b, consist of a broad band with two emission maxima

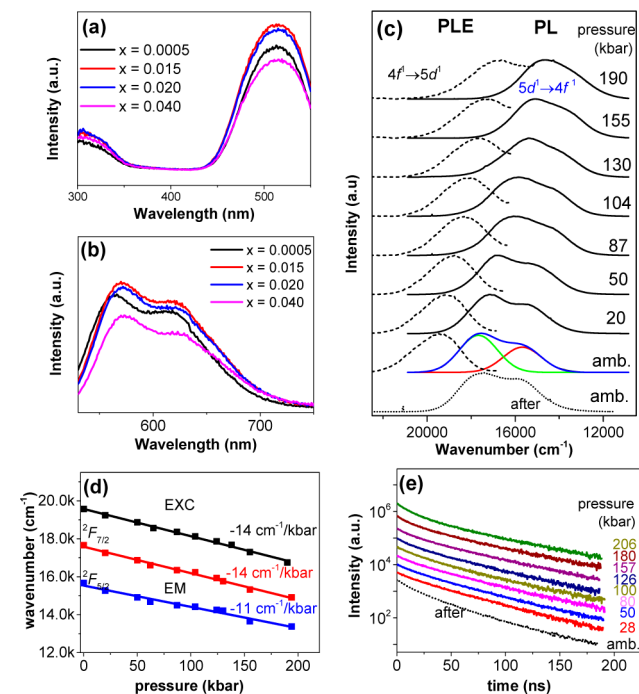


**Figure 2.** (a) Photoluminescence excitation monitored at 580 nm. (b) Photoluminescence after  $\lambda_{\text{exc}} = 460$  nm, and (c) PLE and PL spectra of  $\text{Sr}_{0.985}[\text{Mg}_2\text{Al}_2\text{N}_4]:\text{Ce}_{0.015}^{3+}$  under high hydrostatic pressure ( $\lambda_{\text{exc}} = 510$  nm). (d) Energies of the excitation and emission peaks of  $\text{Sr}_{0.985}[\text{Mg}_2\text{Al}_2\text{N}_4]:\text{Ce}_{0.015}^{3+}$  vs pressure (red/blue squares, maxima of  $\text{Ce}^{3+}$  emission,  $5d^1(^2E) \rightarrow 4f^1(^2F_{5/2}, ^2F_{7/2})$  transitions; black squares, maxima of PLE band ( $4f^1 \rightarrow 5d^1$ ) position under different pressures. (e) Decay curves of  $\text{Sr}_{0.985}[\text{Mg}_2\text{Al}_2\text{N}_4]$ .

of similar intensities, due to the transitions from the lowest 5d level to  $^2F_{7/2}$  and  $^2F_{5/2}$  states of the ground electronic configuration ( $4f$ ). The  $\text{Ce}^{3+}$  replaces the  $\text{Sr}^{2+}$  and is 8-fold coordinated by nitrogen forming a cuboid-like polyhedron.<sup>5</sup> This is similar to  $\text{Ce}^{3+}$  replacing  $\text{Y}^{3+}$  in  $\text{Y}_3\text{Al}_5\text{O}_{12}$  (YAG), where the crystal field causes the splitting of the 5d electronic manifold into the lower doubly degenerate  $^2E$  state and higher triply degenerate  $^2T_2$  state.<sup>8</sup> The electron–lattice interaction diminishes additionally the energy of the  $^2E$  electronic manifold that results in the appearance of homogeneously broadened luminescence band related to  $5d^1(^2E) \rightarrow 4f^1(^2F_{7/2}, ^2F_{5/2})$  transitions.<sup>9,10</sup> In  $\text{Sr}[\text{Mg}_2\text{Al}_2\text{N}_4]$ , the center of gravity of 5d states is at a much lower energy than in oxides due to the higher formal charge of  $\text{N}^{3-}$  compared to  $\text{O}^{2-}$ . As  $\text{Ce}^{3+}$  replaces the larger  $\text{Sr}^{2+}$ , the coordination polyhedron would tend to shrink if its shape is undistorted. With increasing  $\text{Ce}^{3+}$  doping, albeit small, the crystal field may also increase if 5d energy centroid remains nearly unchanged. Further, the lower electronegativity of nitrogen compared to oxygen causes a greater nephelauxetic effect.<sup>5,9</sup> An additional broadening of the  $\text{Ce}^{3+}$  luminescence in  $\text{Sr}[\text{Mg}_2\text{Al}_2\text{N}_4]$  arises from the inherent disordering of the cations in the tetrahedral domains (i.e., Mg and Al). This situation provides for the varying Al–N and Mg–N distances within the tetrahedral framework, coupled with the nature of  $\text{Ce}^{3+}$  emission and inevitably the varying Ce–N distances and coordination environment. Induced in this way,

variable crystal field strength causes variable energy of the emitting  ${}^2E$  state and the further broadening of the emission band. This effect is corroborated in contrast by the narrow emission bands of the ordered  $UCr_4C_4$ -type, such as  $Sr[LiAl_3N_4]$ ,  $Ca[LiAl_3N_4]$ , or  $Sr[Mg_3SiN_4]$ .<sup>1,2,4</sup> It should be noted that the inhomogeneous broadening is responsible for narrowing of the luminescence bands seen after 460 nm excitation (Figure S4c). Only a part of the  $Ce^{3+}$  ions is excited that causes the narrowing of the luminescence band. The internal quantum efficiency, IQE, (Figure S5) of  $\sim 35\%$  for  $x = 0.015$  ( $\lambda_{exc} = 510$  nm) is the best in the series. The phosphor retains  $\sim 65\%$  of its original intensity at  $150$  °C (Figure S6).

The effect of pressure on the luminescence behavior of phosphors is a strategy to evaluate its luminescence dynamics and behavior. Increasing pressure causes the red shift of the PLE and PL spectra, whereas spectral profiles are not significantly altered. The PL spectra were decomposed into two Gaussian bands (which have the same widths), which are related to the transition from the  $5d^1$  ( ${}^2E$ ) excited state to the  ${}^2F_{7/2}$  and  ${}^2F_{5/2}$  states of the ground electronic configuration  $4f^1$  of  $Ce^{3+}$  (Figure 2c). The positions of the peaks versus pressure are shown in Figure 2d. The energetic distance between  ${}^2F_{5/2}$  and  ${}^2F_{7/2}$  slightly decreases under pressure. However, after releasing the pressure, the emission spectrum reverts to its original position. The decay curves of  $Sr_{1-x}[Mg_2Al_2N_4]:Ce_x^{3+}$  ( $x = 0.015$ ) under different pressure condition are shown in Figure 2e reveals that under pressure become multiexponential with the appearance of faster components. In contrast to the luminescence line shape after releasing the pressure, the decay profile differs from that observed before the application of pressure, and the decay time is shorter which is accounted for by pressure-induced appearance of new channels of non-radiative deactivation. Further, the Ce  $L_3$ -edge XANES standard spectra indicate that  $Ce^{3+}$  and  $Ce^{4+}$  coexist in  $Sr[Mg_2Al_2N_4]$  although higher  $Ce^{3+}/Ce^{4+}$  is noted at lower  $x$  values. XANES at the Ce  $L_3$ -edge involves the electronic transition from Ce 2p to outermost shell 4f5d6s level and has been widely used to study the electronic configurations of Ce.<sup>11</sup> Hence, more  $Ce^{3+}$  exists when concentration is  $x = 0.02$  than when  $x$  is more. This behavior accounts for the observed higher intensity emission and the optimum  $Ce^{3+}$  loading.

The  $Sr_{0.985}[Mg_2Al_2N_4]:Ce_{0.015}^{3+}$  was used to generate white LED (Figure 3b), as employed in a package using a prefabricated blue chip LED and  $\beta$ -SiAlON as green phosphor. By varying the relative amount (by wt) of  $\beta$ -SiAlON and

$Sr_{0.985}[Mg_2Al_2N_4]:Ce_{0.015}^{3+}$ , one can tune the white light (Table S4, Figure S8). The stepwise coating of the blue chip with the green phosphor ( $\beta$ -SiAlON) then the  $Sr[Mg_2Al_2N_4]:Ce^{3+}$  (Figure 3a) took into consideration the latter's more effective excitation by green light. This assembly circumvented the usual three-phosphor LEDs excited by the blue chip to generate white light (Figure 3b). In the configuration of the LED package (Figure 3b), the blue LED was allowed to excite the  $\beta$ -SiAlON:Eu $^{2+}$  in the package, which results in the production of green light emission. Consequently, this green light excited  $Sr_{0.985}(Mg_2Al_2N_4):Ce^{3+}$ , exhibiting its yellow emission. This broad emission of the  $Sr_{0.985}(Mg_2Al_2N_4):Ce^{3+}$  spans up to the longer wavelength region (red), thereby covering a wider range in the visible spectrum thus, enabling the generation of white light (inset, Figure 3c). This configuration provides an opportunity for the application of the  $Ce^{3+}$ -doped  $Sr[Mg_2Al_2N_4]$  phosphor toward the generation of white light (CIE  $x = 0.3522$ ,  $y = 0.3279$ , correlated color temperature = 4595 K,  $R_a = 61$ , efficacy = 20 lm/W) in a two-component pc-LED package (Table S5).

In conclusion, we prepared a  $Ce^{3+}$ -doped nitridomagnesoaluminate  $Sr[Mg_2Al_2N_4]$  phosphor from all-nitride precursors using GPS. The phosphor is effectively excitable by green light (510 nm). Homogeneous and inhomogeneous broadening is responsible for appearance of broad luminescence that cover the spectral region from 500 to 700 nm with maximum emissions at 580 and 620 nm. Pressure-dependent luminescence results show the significant red shift of the luminescence and excitation bands (equal to  $14$   $cm^{-1}/kbar$ ) and reveal the presence of additional pathway for nonradiative deactivation. The  $Sr_{0.985}[Mg_2Al_2N_4]:Ce_{0.015}^{3+}$  phosphor retained  $\sim 65\%$  of its intensity at  $150$  °C. With a blue LED excitable pc-LED package, where it is coated on top of the  $\beta$ -SiAlON:Eu $^{2+}$ -coated blue LED chip and white light with CCT = 4595 K and  $R_a = 61$  with 20 lm/W efficacy was generated. This  $Ce^{3+}$ -doped phosphor demonstrates how it can substitute for the emission of two phosphors. With its green-excitability property, the sequential coating rather than mixing the phosphors enables the generation of white light.

## ■ ASSOCIATED CONTENT

### 📄 Supporting Information

The Supporting Information is available free of charge on the ACS Publications website at DOI: 10.1021/acs.chemmater.6b03442.

Experimental details; crystallographic data; LED package performance; crystal structure; SXRD; photoluminescence; quantum efficiency; TEM, SAED and SEM images; electroluminescence, mechanism (PDF)

## ■ AUTHOR INFORMATION

### ✉ Corresponding Author

\*Ru-Shi Liu. E-mail: rslu@ntu.edu.tw.

### Author Contributions

<sup>†</sup>These authors contributed equally.

### Notes

The authors declare no competing financial interest.

## ■ ACKNOWLEDGMENTS

This work was supported by the Ministry of Science and Technology of Taiwan (Contract Nos. MOST 104-2113-M-002-012-MY3, MOST 104-2119-M-002-027-MY3, MOST 104-

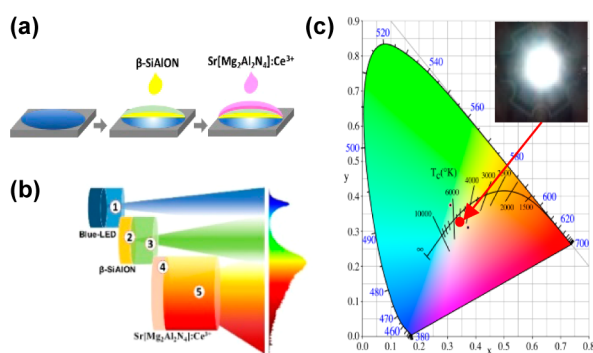


**Figure 3.** White-LED package. (a) Preparation of the LED package through sequential loading of the phosphor slurries. (b) LED assembly showing the green light-excitable  $Sr_{0.985}[Mg_2Al_2N_4]:Ce_{0.015}^{3+}$ . (c) Correlated color temperature 4595 K (inset: sample white light).



2923-M-002-007-MY3); the National Center for Research and Development Poland Grant (No. PL-TW2/8/2015). The contribution of S.M. was supported by the grant "Iuventus Plus" 0271/IP3/2015/73 from Ministry of Science and Higher Education, Poland, and the Russian Foundation for Basic Research (15-52-53080). We also acknowledge the financial support from the Epistar Company. Further details of the crystal structure may be obtained from Fachinformationszentrum Karlsruhe, 76344 Eggenstein-Leopoldshafen, Germany (Fax: (+49)7247-808-666; E-mail: [crystdata@fiz-karlsruhe.de](mailto:crystdata@fiz-karlsruhe.de); [http://www.fiz-karlsruhe.de/request\\_for\\_deposited\\_data.html](http://www.fiz-karlsruhe.de/request_for_deposited_data.html) on quoting the deposition number: CSD-431335.

## REFERENCES

- (1) Li, G.; Tian, Y.; Zhao, Y.; Lin, J. Recent Progress in Luminescence Tuning of Ce<sup>3+</sup> and Eu<sup>2+</sup>-activated Phosphors for pc-WLEDs. *Chem. Soc. Rev.* **2015**, *44*, 8688–8713.
- (2) Pust, P.; Weiler, V.; Hecht, C.; Tucks, A.; Wochnik, A. S.; Henß; Wiechert, D.; Scheu, C.; Schmidt, P. J.; Schnick, W. Narrow-band Red-emitting Sr[LiAl<sub>3</sub>N<sub>4</sub>]:Eu<sup>2+</sup> as a next-generation LED-phosphor material. *Nat. Mater.* **2014**, *13*, 891–896.
- (3) Xia, Z.; Ma, C.; Molokeev, M.; Liu, Q.; Rickert, K.; Poepplmeier, K. R. Chemical Unit Co-substitution and Tuning of Photoluminescence in the Ca<sub>2</sub>(Al<sub>1-x</sub>Mg<sub>x</sub>)(Al<sub>1-x</sub>Si<sub>1+x</sub>)O<sub>7</sub>:Eu<sup>2+</sup> Phosphor. *J. Am. Chem. Soc.* **2015**, *137*, 12494–12497.
- (4) Pust, P.; Hintze, F.; Hecht, C.; Weiler, V.; Locher, A.; Zitnanska, D.; Harm, S.; Wiechert, D.; Schmidt, P.; Schnick, W. Group (III) Nitride M[Mg<sub>2</sub>Al<sub>2</sub>N<sub>4</sub>] (M = Ca, Sr, Ba, Eu) and Ba[Mg<sub>2</sub>Ga<sub>2</sub>N<sub>4</sub>]-Structural Relation and Nontypical Luminescence Properties of Eu<sup>2+</sup>-doped samples. *Chem. Mater.* **2014**, *26*, 6113–6119.
- (5) Xia, Z.; Xu, Z.; Chen, M.; Liu, Q. Recent developments in the new inorganic solid-state LED phosphors. *Dalton Trans.* **2016**, *45*, 11214–11232.
- (6) Park, D. G.; Dong, Y.; Di Salvo, F. J. Sr(Mg<sub>3</sub>Ge)N<sub>4</sub> and Sr(Mg<sub>2</sub>Ga<sub>2</sub>)N<sub>4</sub>: New Isostructural Mg-containing Quaternary Nitrides with Nitridometallate Anions of <sup>3</sup><sub>∞</sub>[(Mg<sub>3</sub>GeN<sub>4</sub>)<sup>2-</sup> and <sup>3</sup><sub>∞</sub>[Mg<sub>2</sub>Ga<sub>2</sub>N<sub>4</sub>]<sup>2-</sup> in a 3D-network Structure. *Solid State Sci.* **2008**, *10*, 1846–1852.
- (7) Greer, H. F.; Zhou, W. Z. Electron Diffraction and HRTEM Imaging of Beam-sensitive Materials. *Crystallogr. Rev.* **2011**, *17*, 163–185.
- (8) Grinberg, M.; Barzowska, J.; Tsuboi, T. *Radiat. Eff. Defects Solids* **2003**, *158*, 39–47.
- (9) van Krevel, J. W. H.; van Rutten, J. W. T.; Mandal, H.; Hintzen, H. T.; Metselaar, R. Luminescence Properties of Terbium-, Cerium-, or Europium-doped α-SiAlON Materials. *J. Solid State Chem.* **2002**, *165*, 19–24.
- (10) Grinberg, M.; Shen, Y. R.; Barzowska, J.; Meltzer, R. S.; Bray, K. L. Pressure Dependence of Electron-Phonon Coupling in Ce<sup>3+</sup>-doped Gd<sub>3</sub>Sc<sub>2</sub>Al<sub>3</sub>O<sub>12</sub> Garnet Crystals. *Phys. Rev. B: Condens. Matter Mater. Phys.* **2004**, *69*, 205101-1–205101-5.
- (11) Xu, F.; Sourty, E.; Shi, W.; Mou, X.; Zhang, L. Direct Observation of Rare-earth Ions in α-SiAlON:Ce<sup>3+</sup> Phosphors. *Inorg. Chem.* **2011**, *50*, 2905–2910.